iScience

Article

Alpha oscillations mediate inhibitory control and perceptual transitions during binocular rivalry

Graphical abstract

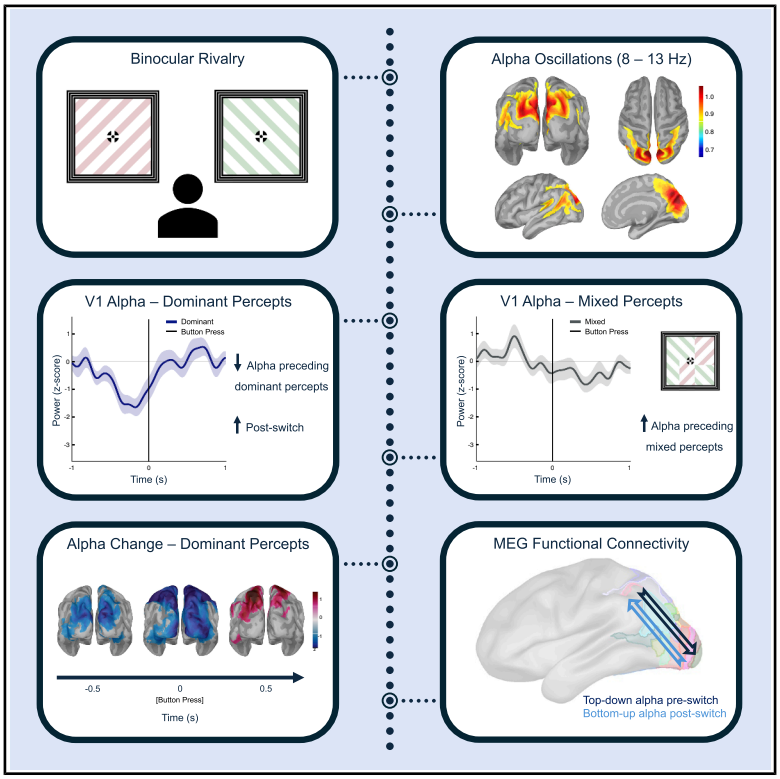

Highlights

- Reduced alpha band power precedes dominant percepts during binocular rivalry
- Increased alpha band power precedes mixed percepts
- Time-resolved alpha power is associated with percept duration
- dPTE reveals distinct patterns of alpha feedback and feedforward connectivity

Authors

Eric Mokri, Jason da Silva Castanheira, Sylvain Baillet, Janine D. Mendola

Correspondence

eric.mokri@mail.mcgill.ca (E.M.), janine.mendola@mcgill.ca (J.D.M.)

In brief

Neuroscience; Sensory neuroscience; Cognitive neuroscience

Mokri et al., 2025, iScience *28*, 113383
September 19, 2025
https://doi.org/10.1016/j.isci.2025.113383

CellPress

iScience

CellPress
OPEN ACCESS

Article

Alpha oscillations mediate inhibitory control and perceptual transitions during binocular rivalry

Eric Mokri,[1,*] Jason da Silva Castanheira,[2] Sylvain Baillet,[2] and Janine D. Mendola[1,3,*]
[1]Department of Ophthalmology & Visual Sciences, McGill University, Montreal, QC H4A 3S5, Canada
[2]McConnell Brain Imaging Centre, Montreal Neurological Institute, McGill University, Montreal, QC H3A 2B4, Canada
[3]Lead contact
*Correspondence: eric.mokri@mail.mcgill.ca (E.M.), janine.mendola@mcgill.ca (J.D.M.)
https://doi.org/10.1016/j.isci.2025.113383

SUMMARY

Binocular rivalry is a visual phenomenon that involves alternating percepts despite stable input, providing a window into perceptual processing and neural dynamics. We examined changes in alpha band activity (8–13 Hz) using magnetoencephalographic imaging (MEG). Our time-frequency analysis demonstrates a decrease in alpha band power before the onset of rivalry alternations, indicating a reduction in inhibitory processing, permitting destabilization of the dominant percept. In contrast, an increase in alpha power was observed prior to participant's report of mixed percepts, suggesting heightened inhibitory processing associated with perceptual ambiguity. Directed connectivity analysis (phase transfer entropy) revealed enhanced feedback connectivity from parietal to early visual areas preceding perceptual dominance, which shifted toward feedforward connectivity following perceptual alternations. These findings suggest that alpha oscillations play a critical role in the excitation-inhibition balance that underlies perceptual stability during binocular rivalry and are further related to individual differences in perceptual experiences.

INTRODUCTION

Binocular rivalry (BR) is a visual illusion that elicits multistable perception. It has been used to study the visual system, as it represents an instance where perception changes despite stable, unchanging retinal input. When each eye is shown a dissimilar, nonfusible image, participants report alternation in image dominance and suppression between the two stimuli.[1,2] BR has been extensively studied and characterized behaviorally, initially with a focus on the role of reciprocal monocular inhibition,[1,3,4] and later with more interest in how binocular neurons might contribute to the neural mechanisms of the phenomenon.[5–8] Recent advances have been contributed by electroencephalography (EEG) studies,[9,10] functional magnetic resonance imaging (fMRI),[11,12] simultaneous EEG-fMRI,[13] and frequency-tagged magnetoencephalography (MEG).[14–17] These studies demonstrate that distinct neural mechanisms are involved in dominance and suppression, and a wide expanse of the visual cortex is recruited.

During BR, as dominant percepts alternate, they are marked by shorter transition periods where portions of each percept may be perceived. These periods, often termed mixed or piecemeal percepts, are dynamically perceived and have provided insight into visual processing. Mixed percepts are unique during rivalry as they allow partial information from each eye to be perceived.[18] They are also thought to represent instances of increased interocular inhibition.[19] In addition, recent tristable models of rivalry account for mixed percepts as related to a discrete perceptual state, in addition to the ongoing dominant percepts.[20,21]

For dominant percepts to emerge, in conjunction with attention and excitability of the dominant neural representation, image suppression of the unattended stimuli is required. For this reason, we and others hypothesize that the balance of excitation and inhibition (E:I) is crucial for the experience of BR. Studies in special populations thought to display E:I imbalances such as autism,[22–24] have shown altered BR dynamics, with slower alternation rates and longer mixed percepts. Computational models of rivalry have also emphasized the role of E:I. Thus, converging evidence supports the role of inhibition within the visual system as crucial to multistable perception and alternations in percepts.[25] Indeed, the balance between excitation and inhibition is crucial in the functioning of the visual system.

Rhythmic alpha-band activity (8–13 Hz) is strongly expressed in the parietal and occipital cortices of the human brain,[26–28] and is thought to reflect these inhibitory processes, especially in vision.[29,30] One significant role of alpha oscillations may be to maintain the E:I balance necessary for visual perception stability during BR. Moreover, E:I imbalances may also contribute to differences in sensory processing and perceptual stability,[31] in addition to the observation that it exhibits stable individual differences, analogous to what is known for perceptual alternation rates, i.e., fast versus slow switchers.[32–34] Within this context, alpha activity exerts inhibitory effects,[35–37] with pulsed-inhibition of ongoing visual processing possibly conveyed via oscillatory dynamics.[38] Feedback mechanisms from higher- to lower-order cortical areas along the functional hierarchy of the visual system have also been linked to alpha oscillatory activity,[39] reinforcing their role in inhibitory control[29,30] and distractor inhibition.[40]

Given this background, our current focus is on task-related modulations of alpha activity during binocular rivalry in relation to subjective reports of percepts.

Other studies have directly linked alpha band activity to rivalrous perception, including correlations between the peak frequency of alpha activity over the occipital cortex during BR and the perceptual alternation rate.[41] The peak alpha frequency measured with EEG and MEG during a fixation period prior to visual presentation was also related to the duration of BR percepts, with faster occipital alpha activity predicting shorter percept durations.[28,42] In addition, the phase of occipital alpha oscillatory activity is coupled to gamma (40–80 Hz) bursts,[43] and such phase-amplitude coupling is increased during non-rivalrous vision tasks.[44] Indeed, intracranial recordings during BR in the occipital cortex found a decrease in low frequency power (3–30 Hz) and an increase in high-frequency power (50–130 Hz) prior to percept alternations.[45]

When considering alpha power, time-resolved measures of EEG alpha oscillations during a bistable Necker cube image task found a decrease in alpha power over the parieto-occipital scalp electrodes preceding perceptual reversals and an increase in power during the onset of the new percept.[46] That study also reported that bistable percept duration increased following sleep deprivation which is known to be associated with higher alpha power. Similarly, an increase in EEG alpha band amplitude was positively correlated to percept duration[47] and associated with longer percept durations[48] when viewing ambiguous figures, suggesting its role in percept stabilization. Using an ambiguous motion paradigm and MEG, a decrease in alpha band power was observed in posterior sensors more prominently prior to endogenous reversals.[49] These findings suggest that higher levels of alpha activity are related to the stability of visual percepts and may suppress the switching processes that enable alternations between percepts. However, it remains unclear how unique these findings are, or how the network of occipital, posterior temporal, and parietal areas interact during rivalry. Here, we quantified the changes in alpha activity and studied their relationship with binocular rivalry.

We designed a binocular rivalry task, and a matched, non-rivalrous control condition labeled as BR-replay, to identify fluctuations of alpha activity respectively associated with endogenous (internal) versus exogenous (external) mechanisms of perceptual change (Figure 1). We utilized untagged (i.e., non-flickering) BR images for our experimental rivalry condition to examine naturally occurring neural mechanisms during periods of exclusive perceptual dominance or mixed percepts. These effects were characterized using MEG source imaging constrained to MRI individual structural anatomy and related to individual perceptual reports. We also conducted a directed connectivity analysis to identify cortico-cortical interactions between the hierarchy of visual areas. We hypothesized that a reduction in inhibition, reflected by a decrease of alpha activity, could precede alternations in dominant percepts during BR. Prior to ambiguous periods of mixed

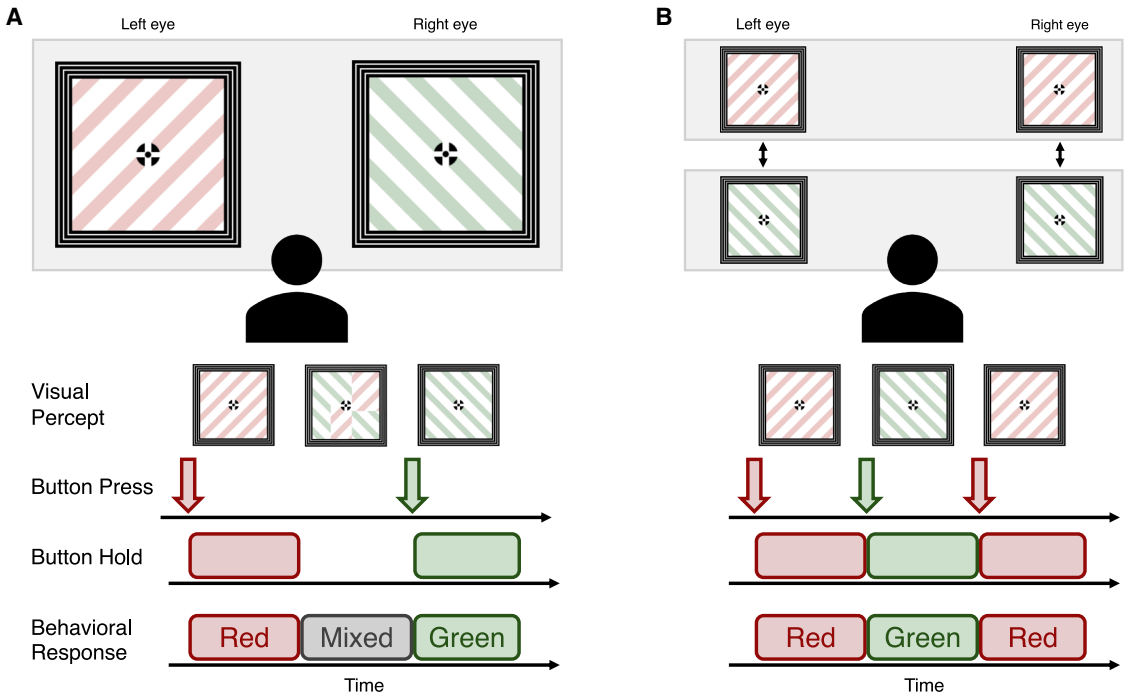

Figure 1. Experimental design

(A) Binocular rivalry condition where each eye is shown either a red or green orthogonal gratings with 90-degree interocular orientation difference. Perception thus alternates between red, green, and mixed percepts, which are reported through a two-button press-and-hold design.

(B) Binocular rivalry replay condition where each eye is shown either matching red or matching green orthogonal gratings. Perception alternated between red and green percepts and participants are tasked with reporting their alternations using a two-button press-and-hold response.

percepts, we expected to observe increases of alpha activity as inhibitory processes would be strongly engaged to stabilize neural processing in a visual system that is temporarily destabilized by conflicting visual information.

RESULTS

Psychophysics

To better characterize the dynamics of perceptual rivalry, we analyzed behavioral aspects of the BR and BR-replay conditions for 28 participants (Table 1), focusing on alternation rates, mean percept durations, and mean viewing proportions (Figure 2). These psychophysics results were derived from rivalry viewing during MEG data acquisition. We also assessed whether the BR-replay condition effectively replicated the BR subjective reports, aiming to identify behavioral differences between dominant and mixed percepts to inform subsequent MEG analysis.

The mean alternation rate (Figure 2A) represents the frequency at which participants transitioned between dominant percepts. This measure is known to be influenced by stimulus properties, image size, and individual differences among participants. The alternation rate, measured in Hertz (Hz), was calculated by dividing the total number of dominant button responses by the experiment duration in seconds (s). The mean alternation rate was 0.41 Hz (SD = 0.12 Hz, 95% confidence interval [CI] = 0.37–0.46 Hz) for the BR condition and 0.41 Hz (SD = 0.017 Hz, 95% CI = 0.40–0.41 Hz) for BR-replay. These results indicate that the BR-replay condition successfully replicated the transition rates observed during traditional BR. Notably, the BR condition exhibited a broader range in the 95% confidence interval and higher standard deviation, suggesting variability in alternation rates across participants.

Mean percept durations were analyzed for both dominant and mixed percepts during BR (Figure 2B). This measure captures the amount of time each percept was held by participants. Percept durations of both red and green percepts were averaged to produce a comprehensive measure, consistent with the MEG analysis approach. Mixed percept duration represented the transition periods when neither red nor green button responses were selected. The mean duration of dominant percepts during BR was 1.83 s (SD = 0.76 s, 95% CI = 1.54–2.13 s), while mixed percepts had a mean duration of 0.85 s (SD = 0.48 s, 95% CI = 0.67–1.04 s). BR-replay only measured the duration of dominant percepts because mixed percepts were eliminated due to both eyes always seeing identical stimuli. The mean duration of dominant percepts during BR-replay was 2.31 s (SD = 0.13 s, 95% CI = 2.26–2.36 s). BR-replay also provided insight into participants' compliance with the instructions and specificities of the two-button press-and-hold design. Additionally, the mean BR-replay switch time of 0.23 s (SD = 0.17 s, 95% CI = 0.16–0.30 s) measured the duration it took participants to transition between key responses, effectively capturing reaction time between percepts. The software used for the replay condition did not mark the time of stimulus changes shown to participants; thus, we used the estimated switch time to approximate the time it took participants to indicate a change in their response between red and green percepts during the BR task.

Table 1. Participant information demographic and visual screening information for all participants analyzed in the psychophysics and MEG experiments

Age	Sex	Left eye acuity	Right eye acuity	Stereo test	Contact lenses	Dominant hand
22	Female	20/16	20/20	9/9	No	Left
29	Male	20/32	20/32	8/9	No	Right
26	Female	20/20	20/32	9/9	Yes	Right
22	Female	20/20	20/25	8/9	No	Right
24	Female	20/20	20/20	9/9	No	Right
22	Female	20/16	20/16	9/9	No	Right
29	Male	20/25	20/25	8/9	No	Right
25	Female	20/25	20/25	9/9	No	Right
29	Male	20/20	20/16	9/9	No	Right
25	Female	20/12.5	20/16	9/9	No	Right
20	Male	20/16	20/16	8/9	No	Right
29	Male	20/16	20/20	9/9	No	Right
21	Male	20/20	20/20	9/9	Yes	Right
30	Female	20/32	20/32	8/9	Yes	Left
24	Female	20/25	20/32	9/9	Yes	Right
24	Female	20/32	20/25	9/9	No	Right
24	Male	20/16	20/16	9/9	No	Right
20	Female	20/20	20/25	9/9	Yes	Right
21	Female	20/16	20/16	9/9	No	Right
22	Female	20/16	20/20	9/9	No	Left
25	Female	20/25	20/25	8/9	No	Right
27	Male	20/25	20/16	9/9	No	Right
24	Male	20/16	20/16	9/9	No	Right
25	Female	20/25	20/16	9/9	No	Right
21	Female	20/16	20/16	9/9	No	Right
26	Female	20/20	20/20	9/9	No	Right
21	Female	20/16	20/12.5	9/9	No	Right
22	Female	20/20	20/16	9/9	No	Left

The information was obtained during the initial screening prior to both psychophysical and MEG experiments for 28 participants.

Mean percept predominance (Figure 2C) served as a measure of the overall viewing proportion of each percept, offering a broader perspective of the BR experience. This measure was calculated by dividing the total time each percept (red, green, or mixed) was reported by the duration of the experiment. During BR, the reported ratios among the three perceptual states were approximately equal. Red was reported with a predominance of 0.36 (SD = 0.10, 95% CI = 0.32–0.40), slightly higher than green with a predominance of 0.33 (SD = 0.097, 95% CI = 0.29–0.37). Mixed percepts were reported with a predominance of 0.30 (SD = 0.20, 95% CI = 0.23–0.38). During BR-replay, the expected ratio between red and green percepts was 1:1, with a small proportion of switch time due to transitions between responses. Red had a predominance of 0.47 (SD = 0.030, 95% CI = 0.46–0.48), green also had a predominance of 0.47 (SD = 0.031, 95% CI = 0.46–0.48), and the switch predominance was 0.057 (SD = 0.062, 95% CI = 0.033–0.081).

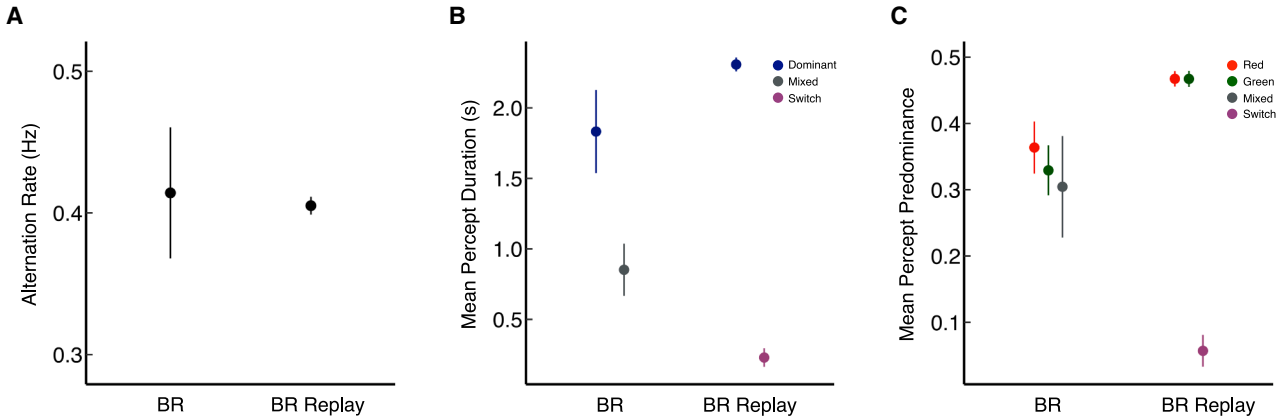

Figure 2. Psychophysics

(A) Mean alternation rate (Hz) for BR and BR-replay conditions with 95% confidence intervals.

(B) Mean duration (seconds) of percepts during for BR and BR-replay conditions with 95% confidence intervals.

(C) Mean proportion of percepts experienced during BR and BR-replay conditions with 95% confidence intervals. The plots show the group means across 28 participants (n = 28).

Overall, our BR-replay condition matched the alternation rate experienced by participants during BR, both having a mean rate of 0.41 Hz. Additionally, we observed task compliance in the proportion and duration of mixed percepts during the replay condition. The expected duration of dominant percepts during the replay condition was 2.50 s, and we observed a mean duration of dominant percepts of 2.31 s, with the difference attributed to slight human error and reaction time. The replay condition did not include image presentations for mixed percepts, thus, we attribute the mean viewing proportion of mixed percepts (0.057), and their duration (230 ms) to the switch time for participants to change between dominant button-press responses during the task.

Alpha activity during binocular rivalry

Prior to conducting event-related analysis of alpha band activity, we examined characteristics of alpha oscillations across the entire BR task. This preliminary analysis aimed to quantify the strength and cortical topography of alpha oscillatory signal during the BR task (Figure 3A). Additionally, we explored the variability and individual differences in the frequency and peak alpha band power across participants (Figure 3B) to determine the range for later analysis. As expected, the strongest evoked signal was localized in the posterior occipito-parietal cortex.

For overall alpha band topography, the data were bandpassed in the alpha range of 8–13 Hz, and time-frequency decomposition was performed using Hilbert transform for each of the 75-s testing blocks to extract the mean power over the duration of the recording. These mean power values were then averaged across the four testing blocks to obtain a group-level result, depicted in Figure 3A. The strongest alpha band power during BR was observed in the posterior cortex, especially the parietal and occipital regions, including activity near and bordering the parieto-occipital sulcus (POS).

Within the primary visual cortex (V1) we used spectral parametrization (specparam) to isolate the periodic peak components (i.e., frequency and amplitude) of the power spectrum during BR.[50] Power spectrum density (PSD) was computed using the Welch method (window length of 3 s and 50% overlap ratio), and specparam measures to isolate periodic spectral components. The mean scout function was utilized to average signals from both the right and left primary visual cortices (V1). We investigated a frequency range of 1–26 Hz to identify a single peak corresponding to the alpha band (8–13 Hz) during BR. We set specparam's hyperparameters to detect a single peak with a minimum height of 0.3 decibels (dB) and width limits of 0.5–3 Hz. We identified a single peak corresponding to the alpha band (8–13 Hz) during BR (Figure 3B). Individual differences in the intensity, shape, and peak frequency of alpha band were observed. The periodic components of the peak alpha band power were observed at a mean frequency of 10.48 Hz (SD = 0.76 Hz), with a mean log power of 5.46 dB (SD = 1.86 dB).

Event-related cortical responses

Event-related analyses aimed to investigate fluctuations in alpha band activity time-locked to perceptual switches during BR and BR-replay dominant percepts, focusing on pre- and post-alternation periods, centered around perceptual switch events. The goal was to localize both spatial and temporal changes in alpha band power during perceptual alternations.

Hilbert transform time-frequency analysis was performed for dominant percepts during BR. MEG data were segmented from −3 to 3 s around each button press, with results extracted between −1 and 1 s to minimize edge effects. Figure 4 (see also Video S1) shows the posterior cortex view, where most event-related changes occurred. The first significant cluster (negative Z score) in alpha power appeared in mid-level visual regions (V3A, V3B, and V4) at −750 ms (Figure 4A). This reduction in power expanded spatially over time, covering much of the posterior cortex. Following the onset of a new dominant percept, alpha power decreased near the motor cortex before a shift toward positive Z score clusters in parietal regions and areas lateral to the primary visual cortex.

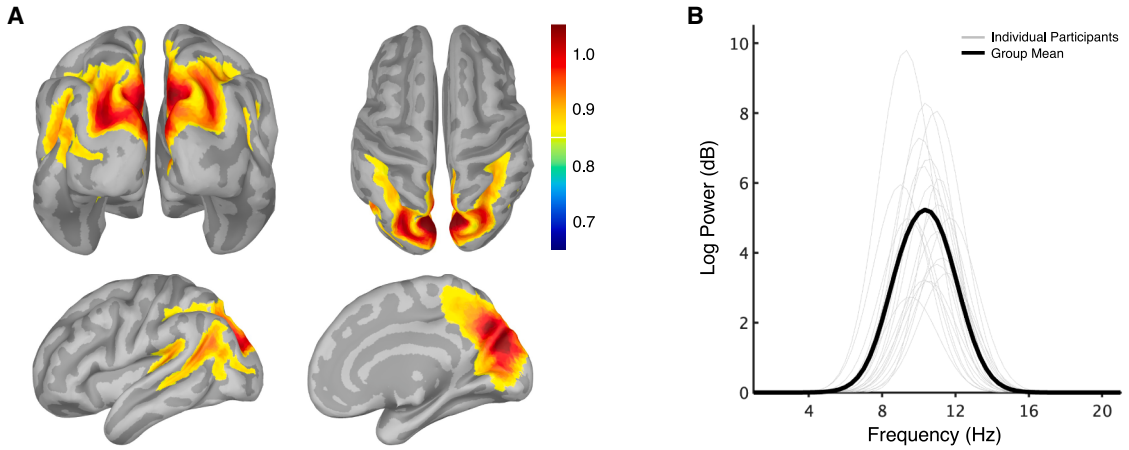

Figure 3. Origins of alpha activity during binocular rivalry

(A) Full cortex view of mean alpha band power during binocular rivalry across all participants ($n = 28$). The cortices are displayed on the 306716V default anatomy cortical surface with parameters set at a 60% smooth surface, a color scale threshold of 50% and a minimum cluster size of 600.

(B) Isolation of alpha peak using spectral parametrization (specparam). Light gray lines indicate individual participant alpha peaks; the group mean is shown with the thicker black line.

Regions of interest analysis

Hilbert transforms between 8 and 13 Hz were computed for three events: BR dominant percepts, BR mixed percepts, and BR-replay dominant percepts. The analysis shown in Figure 5 focused on primary visual cortex responses. During BR dominant percepts (Figure 5A), a decrease in V1 alpha power was observed from −780 ms until 220 ms post-alternation, resulting in a 1 s drop in alpha band power. In the BR-replay condition, alpha power decreased significantly later around −430 ms and returned to baseline at 590 ms post-alternation. A paired t test revealed that the lowest alpha band power prior to dominant percepts (in the time window of −1 to 0.5 s) occurred earlier during rivalry than for BR-replay (t = 2.67, df = 27, $p = 0.013$). The decrease in alpha power prior to the BR dominant condition peaked earlier (M = −204 ms, SD = 351 ms) compared to the BR replay condition (M = −23.8 ms, SD = 349 ms). The mean difference in the latency of the maximal drop in alpha band power was 180 ms, with a moderate effect size (Cohen's d = 0.52).

For mixed percepts during BR, alpha power increased prior to mixed percepts, peaking at −510 ms in V1. A two-tailed paired Student's t test ($\alpha = 0.05$) with FDR correction performed in Brainstorm for the power in V1 revealed significant differences in alpha power between dominant and mixed percepts before the button response. Stronger alpha power was observed prior to mixed percepts within the time window of −427 ms to −115 ms. In contrast, it can also be noted that stronger alpha power was observed for dominant percepts only after the alternation in percept, between the time window from 705 ms to 742 ms.

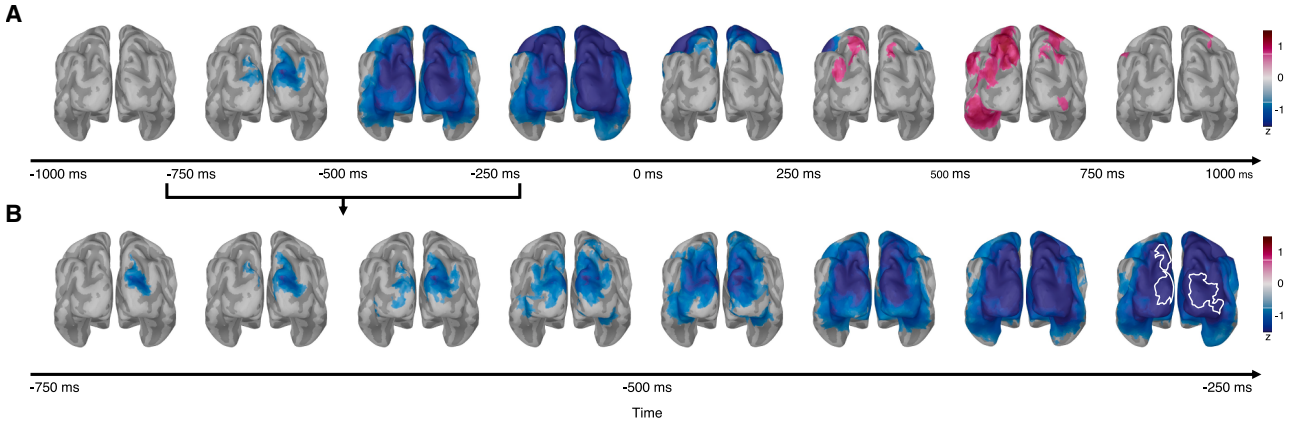

Figure 4. Time-resolved changes in alpha band power during binocular rivalry dominant percepts

(A) Snapshots of group mean ($n = 28$) cortical changes from −1,000 ms to 1,000 ms (in 250 ms intervals), centered on perceptual alternations at time 0 ms.

(B) Snapshots of changes from −750 ms to −250 ms (in 62.5 ms intervals) prior to dominant alternation. Areas of significance ($p < 0.05$) are highlighted in white from the switch time of −230 ms. The cortices are displayed on the 306716V default anatomy cortical surface with parameters set at a 60% smooth surface, a color scale threshold of 50% and a minimum cluster size of 600. See also Video S1.

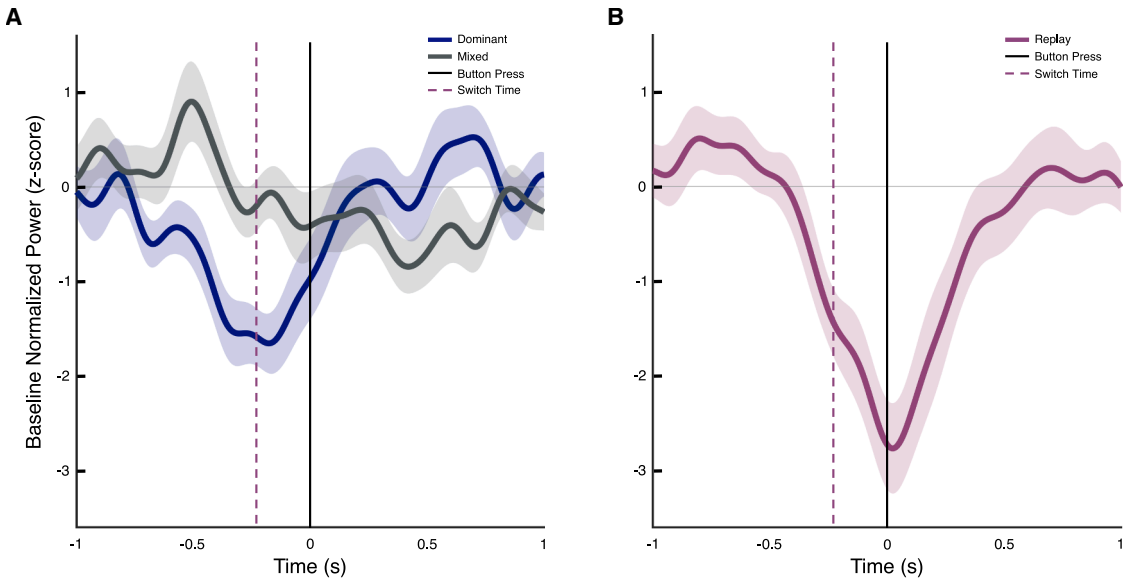

Figure 5. Dynamics of changes in alpha power in primary visual cortex

(A) Baseline normalized (*Z* score) mean alpha power in V1 during BR for dominant and mixed percepts with shaded regions denoting the standard error of the mean (SEM).

(B) Alpha power for BR-replay with shaded region denoting the standard error of the mean (SEM). The report of alternation is identified by the black vertical line and the estimated switch time extracted from the BR replay condition is identified with the dashed vertical line at −230 ms. The data are plotted as the mean of 28 participants (n = 28).

To extend our characterization of alpha power beyond the primary visual cortex, we performed a Hilbert transform time-frequency analysis restricted to the 25 regions of interest (ROI) defined in Table 2. The responses from the right and left hemispheres were averaged for each ROI.

Across the ROIs, we observed a general trend toward a decrease in alpha power preceding dominant percepts during BR (Figure 6A). The onset of the alpha power drop occurred around −700 ms for most regions, with troughs observed prior to the behavioral report of dominant percepts. Not all ROIs showed the same magnitude of change in alpha power. Specifically, early visual areas (i.e., V1, V2, and V3) exhibited the most pronounced decreases, and the strongest negative peak was observed in V3B. Following the button press indicating a dominant percept, we observed a trend toward an increase in alpha power across visual regions. The most prominent positive peaks occurred in higher-level visual regions, including V8/PIT, and other notable peaks were seen in parietal regions such as POS and IP1.

The MEG alpha band activity recorded during BR mixed percepts showed a different overall pattern (Figure 6B). We observed an increase in alpha power prior to the report of a mixed percept, with the strongest response in the posterior occipital cortex (V1/V2) and lateral occipital regions (LO1/LO2 and V4t/LO3). This response began at −700 ms in LO regions, and around −600 ms in V1/V2, peaking near −500 ms (Figures 5A and 6B). Around 300 ms before the report of a mixed percept, and persisting throughout the mixed state, there was a decrease in alpha power. This decrease was most pronounced in the parietal cortex (particularly in areas IP1, IP2, IPS1, and PI). These observed trends in alpha power changes, associated with dominant and mixed percepts reports, provide insights into the underlying neural dynamics, although further statistical analyses are required for a more comprehensive understanding.

Time-resolved correlation analysis—Individual differences

Binocular rivalry is known to exhibit robust individual differences, including variations in percept duration. To investigate the relationship between individual differences in alpha band activity and behavioral outcomes during BR, we conducted a time-resolved correlation analysis between the MEG baseline normalized (*Z* score) alpha band power in V1 extracted from the Hilbert transforms analysis and mean percept durations, separately for dominant and mixed percepts (Figure 7). Non-parametric permutation testing was performed to correct for multiple comparisons. Correlation analysis revealed an extended period, preceding the button press, over which the correlation between alpha band power and mixed percept duration was significant ($p < 0.05$). Significant positive correlations were observed preceding mixed percepts, over a time cluster ranging from −667 ms to −455 ms, and from −282 ms to 208 ms (Figure 7B). For dominant percepts (Figure 7A), for the time periods immediately preceding the response, the correlation between alpha and percept duration was significant over a much shorter window (−212 ms to −148 ms). Another period of significance was observed (−1000 ms to −682 ms), but we consider this period to be well beyond any estimate of reaction time to the button response.

Finally, to provide a visualization that shows individual participant data, we made a scatterplot for the strongest result (mixed percepts) using our estimated switch time of 230 ms preceding

Table 2. Regions of interest generated for each participant for scout-based MEG analysis

Hierarchy	ROI labels	Regions merged from HCP MMP1 atlas
Early		
–	V1*	V1 L and V1 R
	V2*	V2 L and V2 R
	V3*	V3 L and V3 R
Mid-level		
–	V3A	V3A L and V3A R
	V3B	V3B L and V3B R
	V3CD	V3CD L and V3CD R
	V4	V4 L and V4 R
	V6	V6 L and V6 R
	V6A	V6A L and V6A R
	V7	V7 L and V7 R
High-level lateral ventral		
–	LO1/LO2*	LO1 L, LO1 R, LO2 L, and LO2 R
	V4t/LO3*	V4t L, V4t R, LO3 L, and LO3 R
	MT/MST	MT L, MT R, MST L, and MST R
	TPOJ	TPOJ1 L, TPOJ1 R, TPOJ2 L, TPOJ2 R, TPOJ3 L, and TPOJ3 R
	V8/PIT	V8 L, V8 R, PIT L & PIT R
	VMV	VMV1 L, VMV1 R, VMV2 L, VMV2 R, VMV3 L, and VMV3 R
	VVC	VVC1 L and VVC1 R
High-level dorsal		
–	POS	POS1 L, POS1 R, POS2 L, and POS2 R
	IP0*	IP0 L and IP0 R
	IP1*	IP1 L and IP1 R
	IP2*	IP2 L and IP2 R
	IPS1*	IPS1 L and IPS1 R
	PG	PGi L, PGi R, PGp L, PGp R, PGs L, and PGs R
	PI	AIP L, AIP R, LIPd L, LIPd R, LIPv L, LIPv R, MIP L, MIP R, VIP L, and VIP R
	7	7AL L, 7AL R, 7Am L, 7Am R, 7 PC L, 7 PC R, 7 PL L, 7 PL R, 7 P.m. L, 7 P.m. R, 7m L, and 7m R

The regions of interest were mapped for each participant's individual anatomy ($n = 28$). Regions of interest labeled with an asterisk "*" are estimated to be in spatial proximity from previous findings.[51]
The abbreviation L and R refer to right and left hemispheres, respectively.

the response (Figure 7C). We calculated the correlation between alpha power prior to perceptual alternation and the mean percept duration. Baseline normalized alpha power was extracted for each subject in V1 at −230 ms relative to the button press. As expected from the analysis above, a significant positive correlation was found ($t = 2.81$, $df = 24$, p value = 0.0097, $R = 0.50$). The result indicated that participants who demonstrated higher baseline normalized alpha power prior to mixed percepts tended to experience mixed percepts for longer durations.

Alpha band connectivity during binocular rivalry

To further understand the dynamics of alpha band activity during BR dominant percepts, we conducted a directed connectivity analysis using directed phase transfer entropy (dPTE). We used the dPTE to determine the direction of inter-regional influence and computed the normalized result for each region of interest. This resulted in 25 × 25 matrices that show the pairwise relationship between all ROIs (Figure 8). Our aim was to identify patterns of feedback versus feedforward connectivity between ROIs. We further distinguished between pre-dominance and post-dominance alpha band connectivity to compare and contrast their measures.

The dPTE results for both the pre- and post-switch periods (Figures 8A and 8B) indicate that several ROIs exhibited stronger outgoing connections compared to incoming ones, including mid-level regions V3A and V6, and higher-level dorsal regions POS, and area 7. This is evidenced by the consistent horizontal bands observed in Figures 8A and 8B, highlighting these regions as key sources of alpha band activity. Additionally, the weak incoming connections for POS, represented by the distinctly pale vertical band, emphasize its potential role as a causal source of neural signal change.

To further compare pre- and post-switch alpha band connectivity, we computed a difference map (Figure 8C). This analysis showed stronger feedback connectivity—i.e., connectivity from parietal regions to earlier visual areas—during the pre-switch period, indicating an increased influence of parietal areas on the visual system before perceptual dominance was established. In contrast, during the post-switch period, we observed increased feedforward connectivity—i.e., from early visual areas to higher-order visual and parietal areas—suggesting a shift in neural influence after perceptual dominance had been reported.

Statistical analysis was performed to assess significant differences between pre- and post-switch connectivity. The dPTE results in Figures 8A and 8B were found to have a non-normal distribution ($p < 0.05$; Shapiro-Wilk test), so we applied a non-parametric paired-samples permutation test using the Wilcoxon signed-rank method with 10,000 randomizations. The results indicate significant pre-switch feedback influences in green, primarily from higher-level dorsal regions in parietal areas (IP2 and IPS) to early visual areas (V2 and V3), and high-level lateral-ventral regions (lateral occipital and MT/MST). In the post-switch condition, the significant connections—marked in yellow—were predominantly from early (e.g., V2 and V3) and mid-level visual areas (e.g., V3A and V7) to high-level dorsal regions in the parietal cortex, and high-level lateral-ventral regions, highlighting an increased influence of lower visual regions during perceptual dominance.

DISCUSSION

This experiment aimed to understand the influence of alpha band brain oscillations (8–13 Hz) recorded with magnetoencephalography during binocular rivalry. Through time-frequency analysis,

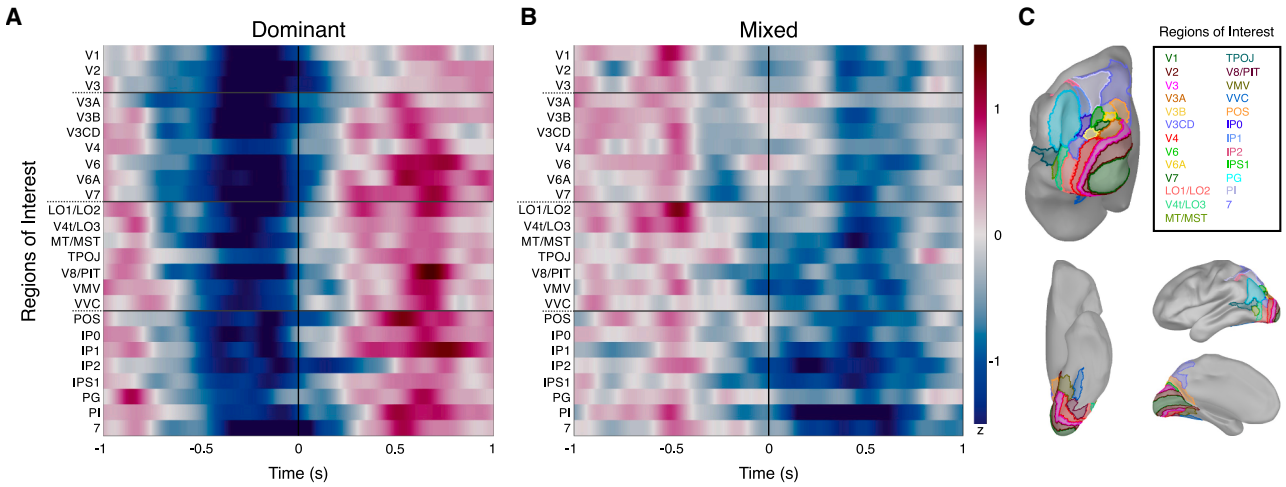

Figure 6. Alpha band spectrogram across regions of interest during binocular rivalry

(A) Time-frequency analysis for BR dominant percepts, centered around the perceptual report indicated by a black vertical line.

(B) Time-frequency analysis for BR mixed percepts, centered around the perceptual report indicated by a black vertical line.

(C) Full cortex visualization of the regions of interest plotted in the Hilbert transform analysis. In (A and B), horizontal lines separate ROIs into hierarchical groups listed in Table 2: early, mid-level, high-level lateral-ventral, and high-level dorsal. The data are plotted as the mean of 28 participants (n = 28).

we consistently observed a decrease in baseline normalized alpha band power starting approximately 1 s before the report of dominant percept alternations during BR. This effect was seen broadly across the visual cortex, covering occipital, temporal, and parietal regions. However, the earliest indicators of decreased power were observed in high- to mid-level visual areas. Notably, the decrease in alpha band power occurred earlier during BR compared to a replay control condition, suggesting differences in underlying neural processes.

We interpret the reduction in alpha band power as reflecting a decrease in inhibitory processing within the visual system, which permits the destabilization of the currently dominant percept and the emergence of the previously suppressed percept, resulting in perceptual alternation. In contrast, mixed percepts were characterized by an increase in alpha band power in visual regions before they were reported. We interpret these changes in the context of excitation-inhibition balance, with our findings highlighting the role of alpha band oscillations in top-down feedback processes during binocular rivalry. Our results contribute to the growing literature on the role of alpha oscillations in human visual perception, particularly during bistable perception.

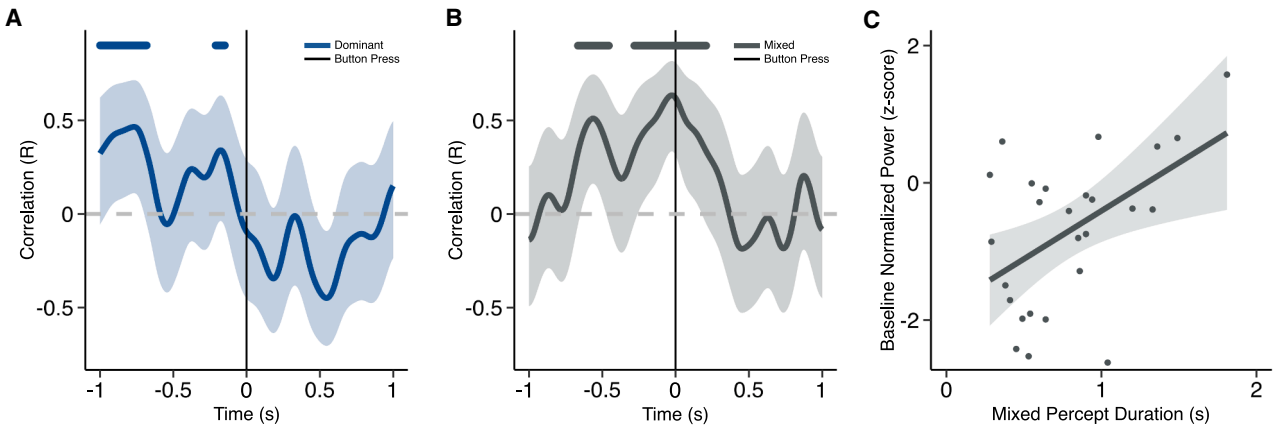

Figure 7. Time-resolved correlation between alpha power and percept duration

(A) Correlation coefficients across the time series for dominant percepts (n = 28). The report of alternation is identified by a black vertical line. Horizontal bars identify significant time points ($p < 0.05$), corrected.

(B) Correlation coefficients across the time series for mixed percepts (n = 27). The report of alternation is identified by a black vertical line. Horizontal bars identify significant time points ($p < 0.05$), corrected.

(C) Scatterplot illustrating the correlation between baseline normalized alpha power in V1 and the mean duration of mixed percepts. Each dot represents individual participants (n = 26). Alpha power was measured 230 ms prior to mixed percept response. The linear line of best fit is shown. Shaded regions represent 95% confidence intervals.

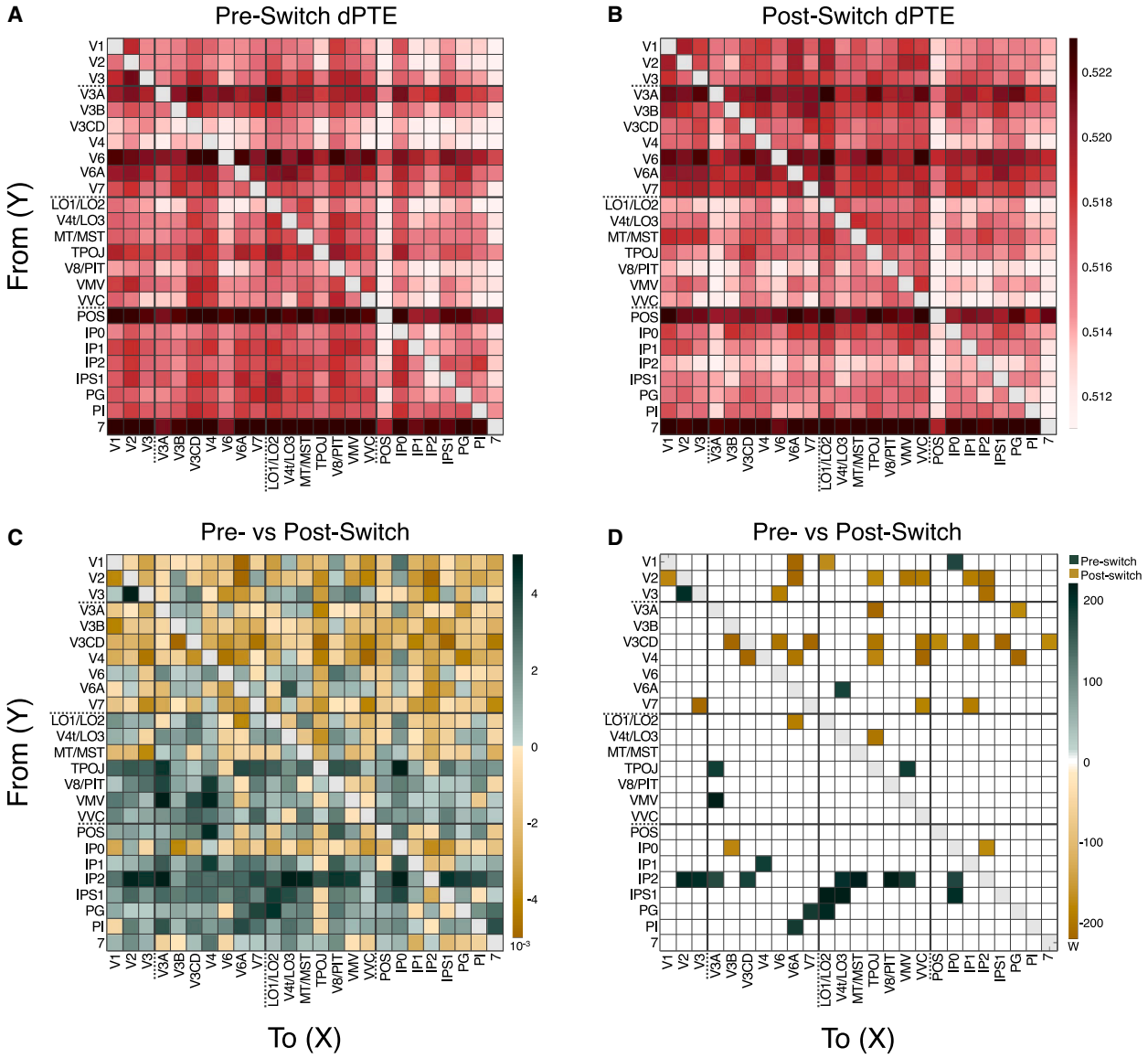

Figure 8. Directed phase transfer entropy analysis for alpha band activity during binocular rivalry dominant percepts

(A) Pre-button press (−1 to 0 s) directed phase transfer entropy (dPTE) alpha band activity.

(B) Post-button press (0 to 1 s) dPTE alpha band activity.

(C) Difference map between pre- and post-button press dPTE (n = 28).

(D) Wilcoxon signed-rank test comparing dPTE connectivity results between pre- and post-switch conditions using paired permutations with 10,000 randomizations. Green squares indicate stronger pre-switch connectivity, while yellow squares indicate stronger post-switch connectivity ($\alpha = 0.05$). In all panels, thicker horizontal and vertical lines separate ROIs into hierarchical groups listed in Table 2: early, mid-level, high-level lateral-ventral, and high-level dorsal. Dashed lines are used for delineation of ROIs along axes. The mean results plotted include 28 participants (n = 28).

Alpha band activity during binocular rivalry

Previous EEG and MEG studies have examined alpha band oscillations during bistable perceptual illusions, such as binocular rivalry.[28,41,42,46] Notably, peak alpha frequency has been found to correlate with alternation rates during BR[41] and during fixation or resting-state periods.[28,42] These findings suggest that alpha oscillations play a role in bistable perception, potentially as a trait-like influence on E:I balance.

Our current findings expand this understanding by focusing on time-locked task changes in alpha power relative to perceptual alternations during BR. Specifically, our MEG results show a decrease in alpha power beginning approximately 750 ms before perceptual alternation, with initial decreases in high- to mid-level visual areas, consistent with earlier EEG findings for bistable stimuli.[46] We also directly compared the BR condition to a replay control condition. During BR, the decrease in alpha band power

began nearly 1 s before perceptual alternation and peaked 175 ms before the switch. By comparison, the alpha power decrease during the replay control peaked 25 ms after the switch, resulting in a temporal shift of 200 ms between conditions. Further, this temporal shift was found to be statistically significant. The inclusion of the replay control condition served to mitigate the effects associated with the voluntary action of initiating a dominant button response.[52] This earlier dip in alpha power during BR likely reflects the neural processing required for endogenous bistable perception and may serve as an early marker of perceptual switching.

Following perceptual dominance during BR, we observed an increase in alpha band power approximately 500 ms after the switch, primarily in the parietal cortex (Figure 4A). We interpret this as indicative of alpha's inhibitory role in maintaining perceptual dominance by suppressing the unattended image and stabilizing the newly dominant percept. However, the dPTE connectivity results show that the balance of feedback compared to feedforward influences diminishes after a switch to dominance.

Additionally, we observed that alpha power changes during the replay control were greater in magnitude than those observed during BR. This could be attributed to the more deterministic alternations in the replay condition, which were unambiguously driven by software. Replay was also tagged (with stimulus flicker) at 5 and 6.67 Hz, with relatively weak harmonics the alpha range. Although this may contribute to the observed magnitude differences for the replay control, it is unlikely to explain the large timing differences between BR and the replay condition. Alpha power is reduced for BR nearly 1 s prior to an alternation and reaches a trough around the estimated decision time of −230 ms, while the trough for the replay control coincides with the button press.

A key finding of our study is the increase in baseline normalized alpha power recorded prior to mixed percepts, which are thought to represent a perceptual state of increased inhibition.[19] These mixed or piecemeal percepts were unique to the BR condition and were not elicited during BR-replay, highlighting their role in perceptual ambiguity (Figure 2C). The strongest increases were observed in early visual regions (V1 and V2) and the lateral occipital areas (LO) approximately 500 ms before the report of a mixed state, suggesting that competitive interactions between excitation and inhibition in these regions play a crucial role in resolving perceptual ambiguity. Indeed, the strength of this alpha peak in the period immediately before the button response was strongly predictive of individual differences in duration of the mixed percepts. Conversely, a decrease in alpha band power was generally observed across the visual system during mixed percepts after the button response (i.e., 0 to 1 s after the button press). Nevertheless, the time-series results revealed a clear dissociation between dominant and mixed percepts. Stronger alpha band power preceded mixed percepts, and this pattern was reversed after the button response, with an increase observed during dominant percepts.

Alpha as an inhibitor in visual perception

Alpha oscillations play a variety of roles across sensory processes, including attention, memory, and perceptual stability.[35–37] In this study, we focused on the inhibitory role of alpha activity within the visual system, where alpha oscillations are known to regulate sensory input and maintain perceptual stability.[29,30] Rivalry arises when ambiguous visual input leads to alternating perceptions without changes in sensory input, highlighting the role of inhibition. Our findings suggest that alpha oscillations are essential in modulating perceptual alternations.

Specifically, we observed a decrease in alpha power prior to perceptual switches, likely reflecting a reduction in inhibitory processing that permits the suppressed percept to gain dominance. This reduction appeared to originate in higher-level visual areas in the parietal cortex, which is known for its role in spatial attention and sensory integration. Our findings also support previous reports of parietal cortex involvement in BR, particularly though transcranial magnetic stimulation (TMS) studies showing causal influence on alternation rates[53,54] and intermittent presentation of BR.[10,55]

These results align with the notion that alpha oscillations act as a gating mechanism, selectively inhibiting competing information to maintain perceptual coherence.[38] This gating mechanism may operate alongside other neural processes governing visual perception and stability. For example, previous studies have observed coupled theta and gamma oscillations during BR, with fronto-medial theta power changes around perceptual alternations.[56,57]

Alpha oscillations also contribute to the E:I ratio, which is crucial for the functioning of the visual system during BR. Imbalances in this ratio, such as those observed in autism,[22–24] are associated with altered BR dynamics, with individuals showing differences in sensory processing and perceptual stability. Our study indicates that individual differences in alpha band power are well associated with the duration of mixed percepts, suggesting that variability in inhibitory control may underlie differences in perceptual experience during bistable perception. Such variability has been shown to have a genetic component, as demonstrated by studies of identical twins.[58,59] A range of other data also supports the premise that measures of E:I ratios show stable individual differences.[32–34]

Models of binocular rivalry

Prevailing views of binocular rivalry have addressed the role of bottom-up (i.e., sensory input driving perception) and top-down (i.e., the role of selective attention) mechanisms of communication. Early models emphasized competition between monocular neurons in early visual areas, driven by mutual inhibition.[1,60] Multistage models[7,61,62] propose that BR involves multiple stages of neural processing, with each stage contributing to competitive interactions. Attention also plays a significant role in rivalry, with research showing its influence on perceptual dominance.[63–66] Future models should consider incorporating brain oscillations, including alpha, to further our understanding of BR dynamics.

Recent MEG studies have provided related insights on the directed connectivity involved in BR. For instance, one study found top-down modulations preceding perceptual dominance, followed by increased bottom-up information flow during BR, although not specific to the alpha band.[67] Another study, using frequency-tagged stimuli to record steady-state visually evoked responses during rivalry, found evidence for feedforward

connectivity during BR and differentiated the mechanisms of dominance and suppression.[17] In contrast, our current analysis of dPTE in the alpha band with untagged (i.e., non-flickering) stimuli revealed increased connectivity from parietal to occipital regions before perceptual dominance, suggesting top-down modulations. Specifically, we interpret the decrease in pre-switch alpha oscillations to be destabilizing and reflect a reduction in top-down inhibition originating from regions in the parietal cortex. The decrease in alpha band activity could affect local E:I balance in multiple visual areas, and reduce net inhibition. This would facilitate the emergence of the previously suppressed percept to become dominant in perception.

After the onset of a dominant percept, connectivity shifted from early visual cortex to higher-level visual and parietal regions, reflecting bottom-up processing which we interpret to provide a stabilizing influence with the increase in alpha band power. This may also serve to facilitate the new dominant percept representation to expand more effectively to higher-level visual regions. Integrating these oscillatory dynamics and connectivity findings into models of binocular rivalry can improve our understanding of the dynamic interplay between sensory input and attentional processes during BR.

In sum, our findings support existing models of BR while highlighting the significant contribution of alpha oscillations to perceptual alternations and stability. Alpha oscillations, through their inhibitory influence, are crucial for shaping the perceptual experience during binocular rivalry, providing a link between sensory processing, attention, and neural oscillatory dynamics.

Limitations of the study

We acknowledge that MEG inherently has limitations in spatial resolution, particularly for resolving deeper subcortical regions. For these analyses of visual cortex, we adhered to state-of-the-art methods and best-practice guidelines for MEG source imaging.[68,69] Our analyses of visual cortical regions benefited from optimal source mapping techniques because they utilized and integrated an individual T1-weighted anatomical MRI for each participant, which significantly improves spatial accuracy. In the visual cortex, previous work demonstrated remarkable accuracy in resolving and distinguishing retinotopic visual areas using MEG.[70]

The findings presented in this paper were obtained from adults within the range of 20–30 years old who reported normal vision and no known visual disorders which could affect generalization to the broader population. Further, the analyses did not consider participant sex as a variable, nor did we collect information on ancestry, race, and ethnicity, which may impact the generalizability of the results. The control condition was frequency tagged at fundamental frequencies that produce weaker self-term harmonics within the alpha frequency band, but we do not believe that this would explain our relevant results. Binocular rivalry is a specific (yet robust) form of bistable perception. The degree to which our observations regarding mixed percepts could extend to other instances of ambiguous percepts is an interesting question for the future. The role of brain oscillations in the alpha frequency band (8–13 Hz) is one of many potential factors contributing to visual perception. Going forward it will be important to strive for integration with previous findings in different frequency bands (i.e., theta, beta, and gamma) and in the coupling between frequency bands between whole-brain regions. Future investigations could also explore the specific role of the periodic versus aperiodic components (i.e., offset and exponent) of the power spectrum and their relationship to behavioral measures of bistable perception,[71] particularly in light of their proposed role in the E:I balance.[72] Finally, the association we suggest here between alpha power and local measures of E:I constitutes correlation not causation. Future studies might address this question more directly with TMS "virtual lesions", MR spectroscopy, or in other clinical populations.

RESOURCE AVAILABILITY

Lead contact

Requests for further information and resources should be directed to and will be fulfilled by the lead contact, Dr. Janine D. Mendola (janine.mendola@mcgill.ca).

Materials availability

This study did not generate new unique reagents.

Data and code availability

- The data were collected from the MEG lab at the McConnell Brain Imaging Center, at McGill University in Montreal, Canada. The original unprocessed MEG data that supported the findings from this paper can be accessed at: https://doi.org/10.5281/zenodo.15802971.
- This paper does not report original code for the MEG analysis. Data analysis was performed with Brainstorm,[73] which is documented and freely available for download online under the GNU general public license (http://neuroimage.usc.edu/brainstorm).
- Any additional information required to reanalyze the data reported in this paper is available from the lead contact upon request.

ACKNOWLEDGMENTS

The MEG lab at the McConnell brain imaging center. Dr. Mathieu Landry for discussion and feedback on the study design. Marc Lalancette for help during the study conceptualization and data acquisition. Dr. Raymundo Cassani for discussion and feedback on MEG connectivity analyses. The study was supported by a Discovery Grant awarded to J.D.M. from the Natural Sciences and Engineering Research Council of Canada (NSERC).

AUTHOR CONTRIBUTIONS

Conceptualization, E.M., J.d.S.C., and J.D.M.; methodology, E.M., J.d.S.C., S.B., and J.D.M.; software, E.M. and J.d.S.C.; formal analysis, E.M.; investigation, E.M. and J.d.S.C.; writing – original draft, E.M. and J.D.M.; writing – review and editing, E.M., J.d.S.C., S.B., and J.D.M.; visualization, E.M. and J.D.M.; supervision, J.D.M; project administration, J.D.M.; funding acquisition, J.D.M.

DECLARATION OF INTERESTS

The authors declare no competing interests.

STAR★METHODS

Detailed methods are provided in the online version of this paper and include the following:

- KEY RESOURCES TABLE
- EXPERIMENTAL MODEL AND STUDY PARTICIPANT DETAILS
  - Human participants
  - Participant screening

SUPPLEMENTAL INFORMATION

Supplemental information can be found online at https://doi.org/10.1016/j.isci.2025.113383.

Received: October 29, 2024
Revised: March 5, 2025
Accepted: August 13, 2025
Published: August 16, 2025

REFERENCES

1. Blake, R. (1989). A neural theory of binocular rivalry. Psychol. Rev. *96*, 145–167. https://doi.org/10.1037/0033-295X.96.1.145.
2. Blake, R., and Logothetis, N.K. (2002). Visual competition. Nat. Rev. Neurosci. *3*, 13–21. https://doi.org/10.1038/nrn701.
3. Matsuoka, K. (1984). The dynamic model of binocular rivalry. Biol. Cybern. *49*, 201–208. https://doi.org/10.1007/BF00334466.
4. Lehky, S.R. (1988). An astable multivibrator model of binocular rivalry. Perception *17*, 215–228. https://doi.org/10.1068/p170215.
5. Logothetis, N.K., Leopold, D.A., and Sheinberg, D.L. (1996). What is rivalling during binocular rivalry? Nature *380*, 621–624. https://doi.org/10.1038/380621a0.
6. Kovács, I., Papathomas, T.V., Yang, M., and Fehér, Á. (1996). When the brain changes its mind: Interocular grouping during binocular rivalry. Proc. Natl. Acad. Sci. USA *93*, 15508–15511. https://doi.org/10.1073/pnas.93.26.15508.
7. Wilson, H.R. (2003). Computational evidence for a rivalry hierarchy in vision. Proc. Natl. Acad. Sci. USA *100*, 14499–14503. https://doi.org/10.1073/pnas.2333622100.
8. Said, C.P., and Heeger, D.J. (2013). A model of binocular rivalry and cross-orientation suppression. PLoS Comput. Biol. *9*, e1002991. https://doi.org/10.1371/journal.pcbi.1002991.
9. Pitts, M.A., Martínez, A., and Hillyard, S.A. (2010). When and where is binocular rivalry resolved in the visual cortex? J. Vis. *10*, 25. https://doi.org/10.1167/10.14.25.
10. Pitts, M.A., and Britz, J. (2011). Insights from intermittent binocular rivalry and EEG. Front. Hum. Neurosci. *5*, 107. https://doi.org/10.3389/fnhum.2011.00107.
11. de Jong, M.C., Kourtzi, Z., and van Ee, R. (2012). Perceptual experience modulates cortical circuits involved in visual awareness. Eur. J. Neurosci. *36*, 3718–3731. https://doi.org/10.1111/ejn.12005.
12. Jamison, K.W., Roy, A.V., He, S., Engel, S.A., and He, B. (2015). SSVEP signatures of binocular rivalry during simultaneous EEG and fMRI. J. Neurosci. Methods *243*, 53–62. https://doi.org/10.1016/j.jneumeth.2015.01.024.
13. Roy, A.V., Jamison, K.W., He, S., Engel, S.A., and He, B. (2017). Deactivation in the posterior mid-cingulate cortex reflects perceptual transitions during binocular rivalry: Evidence from simultaneous EEG-fMRI. Neuroimage *152*, 1–11. https://doi.org/10.1016/j.neuroimage.2017.02.041.
14. Cosmelli, D., David, O., Lachaux, J.P., Martinerie, J., Garnero, L., Renault, B., and Varela, F. (2004). Waves of consciousness: ongoing cortical patterns during binocular rivalry. Neuroimage *23*, 128–140. https://doi.org/10.1016/j.neuroimage.2004.05.008.
15. Kamphuisen, A., Bauer, M., and van Ee, R. (2008). No evidence for widespread synchronized networks in binocular rivalry: MEG frequency tagging entrains primarily early visual cortex. J. Vis. *8*, 1–8. https://doi.org/10.1167/8.5.4.
16. Bock, E.A., Fesi, J.D., Baillet, S., and Mendola, J.D. (2019). Tagged MEG measures binocular rivalry in a cortical network that predicts alternation rate. PLoS One *14*, e0218529. https://doi.org/10.1371/journal.pone.0218529.
17. Bock, E.A., Fesi, J.D., Da Silva Castenheira, J., Baillet, S., and Mendola, J.D. (2023). Distinct dorsal and ventral streams for binocular rivalry dominance and suppression revealed by magnetoencephalography. Eur. J. Neurosci. *57*, 1317–1334. https://doi.org/10.1111/ejn.15955.
18. Alais, D., and Melcher, D. (2007). Strength and coherence of binocular rivalry depends on shared stimulus complexity. Vision Res. *47*, 269–279. https://doi.org/10.1016/j.visres.2006.09.003.
19. Katyal, S., Engel, S.A., He, B., and He, S. (2016). Neurons that detect interocular conflict during binocular rivalry revealed with EEG. J. Vis. *16*, 18. https://doi.org/10.1167/16.3.18.
20. Riesen, G., Norcia, A.M., and Gardner, J.L. (2019). Humans perceive binocular rivalry and fusion in a tristable dynamic state. J. Neurosci. *39*, 8527–8537. https://doi.org/10.1523/JNEUROSCI.0713-19.2019.
21. Qiu, S.X., Caldwell, C.L., You, J.Y., and Mendola, J.D. (2020). Binocular rivalry from luminance and contrast. Vision Res. *175*, 41–50. https://doi.org/10.1016/j.visres.2020.06.006.
22. Robertson, C.E., Kravitz, D.J., Freyberg, J., Baron-Cohen, S., and Baker, C.I. (2013). Slower rate of binocular rivalry in autism. J. Neurosci. *33*, 16983–16991. https://doi.org/10.1523/JNEUROSCI.0448-13.2013.
23. Spiegel, A., Mentch, J., Haskins, A.J., and Robertson, C.E. (2019). Slower binocular rivalry in the autistic brain. Curr. Biol. *29*, 2948–2953.e3. https://doi.org/10.1016/j.cub.2019.07.026.
24. Skerswetat, J., Bex, P.J., and Baron-Cohen, S. (2022). Visual consciousness dynamics in adults with and without autism. Sci. Rep. *12*, 4376. https://doi.org/10.1038/s41598-022-08108-0.
25. Cao, R., Pastukhov, A., Aleshin, S., Mattia, M., and Braun, J. (2021). Binocular rivalry reveals an out-of-equilibrium neural dynamics suited for decision-making. eLife *10*, e61581. https://doi.org/10.7554/eLife.61581.
26. Chapman, R.M., Ilmoniemi, R.J., Barbanera, S., and Romani, G.L. (1984). Selective localization of alpha brain activity with neuromagnetic measurements. Electroencephalogr. Clin. Neurophysiol. *58*, 569–572. https://doi.org/10.1016/0013-4694(84)90047-6.
27. Ciulla, C., Takeda, T., and Endo, H. (1999). MEG characterization of spontaneous alpha rhythm in the human brain. Brain Topogr. *11*, 211–222. https://doi.org/10.1023/A:1022233828999.
28. Katyal, S., He, S., He, B., and Engel, S.A. (2019). Frequency of alpha oscillation predicts individual differences in perceptual stability during binocular rivalry. Hum. Brain Mapp. *40*, 2422–2433. https://doi.org/10.1002/hbm.24533.
29. Jensen, O., Bonnefond, M., Marshall, T.R., and Tiesinga, P. (2015). Oscillatory mechanisms of feedforward and feedback visual processing. Trends Neurosci. *38*, 192–194. https://doi.org/10.1016/j.tins.2015.02.006.
30. Clayton, M.S., Yeung, N., and Cohen Kadosh, R. (2018). The many characters of visual alpha oscillations. Eur. J. Neurosci. *48*, 2498–2508. https://doi.org/10.1111/ejn.13747.
31. Rubenstein, J.L.R., and Merzenich, M.M. (2003). Model of autism: increased ratio of excitation/inhibition in key neural systems. Genes Brain Behav. *2*, 255–267. https://doi.org/10.1034/j.1601-183X.2003.00037.x.
32. Brunel, N., and Wang, X.J. (2003). What determines the frequency of fast network oscillations with irregular neural discharges? I. Synaptic

dynamics and excitation-inhibition balance. J. Neurophysiol. *90*, 415–430. https://doi.org/10.1152/jn.01095.2002.

33. Muthukumaraswamy, S.D., Edden, R.A.E., Jones, D.K., Swettenham, J. B., and Singh, K.D. (2009). Resting GABA concentration predicts peak gamma frequency and fMRI amplitude in response to visual stimulation in humans. Proc. Natl. Acad. Sci. USA *106*, 8356–8361. https://doi.org/10.1073/pnas.0900728106.

34. van Pelt, S., Boomsma, D.I., and Fries, P. (2012). Magnetoencephalography in twins reveals a strong genetic determination of the peak frequency of visually induced gamma-band synchronization. J. Neurosci. *32*, 3388–3392. https://doi.org/10.1523/JNEUROSCI.5592-11.2012.

35. Klimesch, W., Sauseng, P., and Hanslmayr, S. (2007). EEG alpha oscillations: the inhibition–timing hypothesis. Brain Res. Rev. *53*, 63–88. https://doi.org/10.1016/j.brainresrev.2006.06.003.

36. Jensen, O., and Mazaheri, A. (2010). Shaping functional architecture by oscillatory alpha activity: gating by inhibition. Front. Hum. Neurosci. *4*, 186. https://doi.org/10.3389/fnhum.2010.00186.

37. Klimesch, W. (2012). Alpha-band oscillations, attention, and controlled access to stored information. Trends Cogn. Sci. *16*, 606–617. https://doi.org/10.1016/j.tics.2012.10.007.

38. Mathewson, K.E., Lleras, A., Beck, D.M., Fabiani, M., Ro, T., and Gratton, G. (2011). Pulsed out of awareness: EEG alpha oscillations represent a pulsed-inhibition of ongoing cortical processing. Front. Psychol. *2*, 99. https://doi.org/10.3389/fpsyg.2011.00099.

39. Van Kerkoerle, T., Self, M.W., Dagnino, B., Gariel-Mathis, M.A., Poort, J., Van Der Togt, C., and Roelfsema, P.R. (2014). Alpha and gamma oscillations characterize feedback and feedforward processing in monkey visual cortex. Proc. Natl. Acad. Sci. USA *111*, 14332–14341. https://doi.org/10.1073/pnas.1402773111.

40. Bonnefond, M., and Jensen, O. (2025). The role of alpha oscillations in resisting distraction. Trends Cogn. Sci. *29*, 368–379. https://doi.org/10.1016/j.tics.2024.11.004.

41. Torralba Cuello, M., Drew, A., Sabaté San José, A., Morís Fernández, L., and Soto-Faraco, S. (2022). Alpha fluctuations regulate the accrual of visual information to awareness. Cortex *147*, 58–71. https://doi.org/10.1016/j.cortex.2021.11.017.

42. Sponheim, S.R., Stim, J.J., Engel, S.A., and Pokorny, V.J. (2023). Slowed alpha oscillations and percept formation in psychotic psychopathology. Front. Psychol. *14*, 1144107. https://doi.org/10.3389/fpsyg.2023.1144107.

43. Osipova, D., Hermes, D., and Jensen, O. (2008). Gamma power is phase-locked to posterior alpha activity. PLoS One *3*, e3990. https://doi.org/10.1371/journal.pone.0003990.

44. Voytek, B., Canolty, R.T., Shestyuk, A., Crone, N.E., Parvizi, J., and Knight, R.T. (2010). Shifts in gamma phase–amplitude coupling frequency from theta to alpha over posterior cortex during visual tasks. Front. Hum. Neurosci. *4*, 191. https://doi.org/10.3389/fnhum.2010.00191.

45. de Jong, M.C., Hendriks, R.J.M., Vansteensel, M.J., Raemaekers, M., Verstraten, F.A.J., Ramsey, N.F., Erkelens, C.J., Leijten, F.S.S., and Van Ee, R. (2016). Intracranial recordings of occipital cortex responses to illusory visual events. J. Neurosci. *36*, 6297–6311. https://doi.org/10.1523/JNEUROSCI.0242-15.2016.

46. Piantoni, G., Romeijn, N., Gomez-Herrero, G., Van Der Werf, Y.D., and Van Someren, E.J.W. (2017). Alpha power predicts persistence of bistable perception. Sci. Rep. *7*, 5208. https://doi.org/10.1038/s41598-017-05610-8.

47. Zhu, M., Hardstone, R., and He, B.J. (2022). Neural oscillations promoting perceptual stability and perceptual memory during bistable perception. Sci. Rep. *12*, 2760. https://doi.org/10.1038/s41598-022-06570-4.

48. Hardstone, R., Flounders, M.W., Zhu, M., and He, B.J. (2022). Frequency-specific neural signatures of perceptual content and perceptual stability. eLife *11*, e78108. https://doi.org/10.7554/eLife.78108.

49. Strüber, D., and Herrmann, C.S. (2002). MEG alpha activity decrease reflects destabilization of multistable percepts. Cogn. Brain Res. *14*, 370–382. https://doi.org/10.1016/S0926-6410(02)00139-8.

50. Donoghue, T., Haller, M., Peterson, E.J., Varma, P., Sebastian, P., Gao, R., Noto, T., Lara, A.H., Wallis, J.D., Knight, R.T., et al. (2020). Parameterizing neural power spectra into periodic and aperiodic components. Nat. Neurosci. *23*, 1655–1665. https://doi.org/10.1038/s41593-020-00744-x.

51. Cichy, R.M., Pantazis, D., and Oliva, A. (2016). Similarity-based fusion of MEG and fMRI reveals spatio-temporal dynamics in human cortex during visual object recognition. Cereb. Cortex *26*, 3563–3579. https://doi.org/10.1093/cercor/bhw135.

52. Acquafredda, M., Binda, P., and Lunghi, C. (2022). Attention cueing in rivalry: Insights from pupillometry. Eneuro *9*, ENEURO.0497-21.2022. https://doi.org/10.1523/ENEURO.0497-21.2022.

53. Zaretskaya, N., Thielscher, A., Logothetis, N.K., and Bartels, A. (2010). Disrupting parietal function prolongs dominance durations in binocular rivalry. Curr. Biol. *20*, 2106–2111. https://doi.org/10.1016/j.cub.2010.10.046.

54. Carmel, D., Walsh, V., Lavie, N., and Rees, G. (2010). Right parietal TMS shortens dominance durations in binocular rivalry. Curr. Biol. *20*, R799–R800. https://doi.org/10.1016/j.cub.2010.07.036.

55. Britz, J., and Pitts, M.A. (2011). Perceptual reversals during binocular rivalry: ERP components and their concomitant source differences. Psychophysiology *48*, 1490–1499. https://doi.org/10.1111/j.1469-8986.2011.01222.x.

56. Doesburg, S.M., Green, J.J., McDonald, J.J., and Ward, L.M. (2009). Rhythms of consciousness: binocular rivalry reveals large-scale oscillatory network dynamics mediating visual perception. PLoS One *4*, e6142. https://doi.org/10.1371/journal.pone.0006142.

57. Drew, A., Torralba, M., Ruzzoli, M., Morís Fernández, L., Sabaté, A., Pápai, M.S., and Soto-Faraco, S. (2022). Conflict monitoring and attentional adjustment during binocular rivalry. Eur. J. Neurosci. *55*, 138–153. https://doi.org/10.1111/ejn.15554.

58. Miller, S.M., Hansell, N.K., Ngo, T.T., Liu, G.B., Pettigrew, J.D., Martin, N. G., and Wright, M.J. (2010). Genetic contribution to individual variation in binocular rivalry rate. Proc. Natl. Acad. Sci. USA *107*, 2664–2668. https://doi.org/10.1073/pnas.0912149107.

59. Shannon, R.W., Patrick, C.J., Jiang, Y., Bernat, E., and He, S. (2011). Genes contribute to the switching dynamics of bistable perception. J. Vis. *11*. https://doi.org/10.1167/11.3.8.

60. Tong, F. (2001). Competing theories of binocular rivalry: A possible resolution. Brain Mind *2*, 55–83. https://doi.org/10.1023/A:1017942718744.

61. Freeman, A.W. (2005). Multistage model for binocular rivalry. J. Neurophysiol. *94*, 4412–4420. https://doi.org/10.1152/jn.00557.2005.

62. Tong, F., Meng, M., and Blake, R. (2006). Neural bases of binocular rivalry. Trends Cogn. Sci. *10*, 502–511. https://doi.org/10.1016/j.tics.2006.09.003.

63. Zhang, P., Jamison, K., Engel, S., He, B., and He, S. (2011). Binocular rivalry requires visual attention. Neuron *71*, 362–369. https://doi.org/10.1016/j.neuron.2011.05.035.

64. Chong, S.C., and Blake, R. (2006). Exogenous attention and endogenous attention influence initial dominance in binocular rivalry. Vision Res. *46*, 1794–1803. https://doi.org/10.1016/j.visres.2005.10.031.

65. Dieter, K.C., Melnick, M.D., and Tadin, D. (2015). When can attention influence binocular rivalry? Atten. Percept. Psychophys. *77*, 1908–1918. https://doi.org/10.3758/s13414-015-0905-6.

66. Li, H.H., Rankin, J., Rinzel, J., Carrasco, M., and Heeger, D.J. (2017). Attention model of binocular rivalry. Proc. Natl. Acad. Sci. USA *114*, E6192–E6201. https://doi.org/10.1073/pnas.1620475114.

67. Dijkstra, N., van de Nieuwenhuijzen, M.E., and van Gerven, M.A.J. (2016). The spatiotemporal dynamics of binocular rivalry: evidence for increased top-down flow prior to a perceptual switch. Neurosci. Conscious. *2016*, niw003. https://doi.org/10.1093/nc/niw003.

68. Gross, J., Baillet, S., Barnes, G.R., Henson, R.N., Hillebrand, A., Jensen, O., Jerbi, K., Litvak, V., Maess, B., Oostenveld, R., et al. (2013). Good practice for conducting and reporting MEG research. Neuroimage *65*, 349–363. https://doi.org/10.1016/j.neuroimage.2012.10.001.

69. Baillet, S. (2017). Magnetoencephalography for brain electrophysiology and imaging. Nat. Neurosci. *20*, 327–339. https://doi.org/10.1038/nn.4504.

70. Nasiotis, K., Clavagnier, S., Baillet, S., and Pack, C.C. (2017). High-resolution retinotopic maps estimated with magnetoencephalography. Neuroimage *145*, 107–117. https://doi.org/10.1016/j.neuroimage.2016.10.017.

71. Wilson, L.E., da Silva Castanheira, J., and Baillet, S. (2022). Time-resolved parameterization of aperiodic and periodic brain activity. eLife *11*, e77348. https://doi.org/10.7554/eLife.77348.

72. Gao, R., Peterson, E.J., and Voytek, B. (2017). Inferring synaptic excitation/inhibition balance from field potentials. Neuroimage *158*, 70–78. https://doi.org/10.1016/j.neuroimage.2017.06.078.

73. Tadel, F., Baillet, S., Mosher, J.C., Pantazis, D., and Leahy, R.M. (2011). Brainstorm: a user- friendly application for MEG/EEG analysis. Comput. Intell. Neurosci. *2011*, 879716. https://doi.org/10.1155/2011/879716.

74. Brainard, D.H. (1997). The Psychophysics Toolbox. Spat. Vis. *10*, 433–436.

75. Kleiner, M., Brainard, D., and Pelli, D. (2007). What's new in Psychtoolbox-3? Perception *36*, 1–16.

76. Mokri, E., da Silva Castanheira, J., Laldin, S., Landry, M., and Mendola, J. D. (2023). Effects of interocular grouping demands on binocular rivalry. J. Vis. *23*, 15. https://doi.org/10.1167/jov.23.10.15.

77. Thaler, L., Schütz, A.C., Goodale, M.A., and Gegenfurtner, K.R. (2013). What is the best fixation target? The effect of target shape on stability of fixational eye movements. Vision Res. *76*, 31–42. https://doi.org/10.1016/j.visres.2012.10.012.

78. Gaser, C., Dahnke, R., Thompson, P.M., Kurth, F., and Luders, E.; Alzheimer's Disease Neuroimaging Initiative (2022). CAT–A computational anatomy toolbox for the analysis of structural MRI data. Preprint at bioRxiv. https://doi.org/10.1101/2022.06.11.495736.

79. Glasser, M.F., Coalson, T.S., Robinson, E.C., Hacker, C.D., Harwell, J., Yacoub, E., Ugurbil, K., Andersson, J., Beckmann, C.F., Jenkinson, M., et al. (2016). A multi-modal parcellation of human cerebral cortex. Nature *536*, 171–178. https://doi.org/10.1038/nature18933.

80. Szekely, B., Keys, R., MacNeilage, P., and Alais, D. (2024). Binocular rivalry dynamics during locomotion. PLoS One *19*, e0300222. https://doi.org/10.1371/journal.pone.0300222.

81. R Core Team (2024). R: A Language and Environment for Statistical Computing (R Foundation for Statistical Computing). https://www.R-project.org/.

82. Lobier, M., Siebenhühner, F., Palva, S., and Palva, J.M. (2014). Phase transfer entropy: a novel phase-based measure for directed connectivity in networks coupled by oscillatory interactions. Neuroimage *85*, 853–872. https://doi.org/10.1016/j.neuroimage.2013.08.056.

83. Hillebrand, A., Tewarie, P., Van Dellen, E., Yu, M., Carbo, E.W.S., Douw, L., Gouw, A.A., van Straaten, E.C.W., and Stam, C.J. (2016). Direction of information flow in large-scale resting-state networks is frequency-dependent. Proc. Natl. Acad. Sci. USA *113*, 3867–3872. https://doi.org/10.1073/pnas.1515657113.

84. Müller, F., Niso, G., Samiee, S., Ptito, M., Baillet, S., and Kupers, R. (2019). A thalamocortical pathway for fast rerouting of tactile information to occipital cortex in congenital blindness. Nat. Commun. *10*, 5154. https://doi.org/10.1038/s41467-019-13173-7.

STAR★METHODS

KEY RESOURCES TABLE

REAGENT or RESOURCE	SOURCE	IDENTIFIER
Deposited data		
Unprocessed MEG data for BR and BR replay	Zenodo	Zenodo: https://doi.org/10.5281/zenodo.15802971
Behavioral data for BR and BR replay	Zenodo	Zenodo: https://doi.org/10.5281/zenodo.15802971
Software and algorithms		
Brainstorm	Tadel et al.[73]	https://neuroimage.usc.edu/brainstorm/
MATLAB 2021a	MathWorks	https://www.mathworks.com/
R	R Foundation for Statistical Computing	https://www.R-project.org/
Psychtoolbox-3	Brainard[74]; Kleiner et al.[75]	https://psychtoolbox.org/
Other		
Magnetoencephalography	CTF MEG Neuro Innovations, Inc.	https://www.ctf.com/
VPixx projector	VPixx Technologies	https://vpixx.com/
Polhemus Fastrak system	Polhemus	https://polhemus.com/
Logarithmic Visual Acuity chart	Precision Vision	https://precision-vision.com/
Titmus Stereoacuity Test	Stereo Optical	https://www.stereooptical.com/

EXPERIMENTAL MODEL AND STUDY PARTICIPANT DETAILS

Human participants

Thirty-one participants participated in the experimental studies that included an initial day of psychophysics testing,[76] two days of MEG testing, and the acquisition of a structural MRI. Of the thirty-one participants, three were excluded due to issues with the scalp digitization at the time of data acquisition. The analysis was conducted on twenty-eight participants (9 males and 19 females, mean age 24.25 ± 3.00 years with a range between 20 and 30 years). All participants provided informed consent to participate in both the psychophysical and MEG portions of these experiments. This experimental protocol (# 21-10-047) was approved by the McGill University Faculty of Medicine and Health Sciences (FMHS) Research Ethics Office (IRB).

Participant screening

Participant were screened on the initial day of testing. The initial screening during recruitment included normal or corrected-to-normal vision, no visual disorders, no metal implants, and not taking psychoactive nor psychotropic medication. Participants were permitted to wear contact lenses or have undergone eye correction surgery, and their glasses were replaced with MEG-compatible prism lenses. Prior to testing, participants were screened for visual acuity and stereo vision. Visual acuity was assessed using the Logarithmic Visual Acuity chart (Early Treatment Diabetic Retinopathy Study [ETDRS] 2000 series chart; Precision Vision, Woodstock, IL) with an inclusion criteria of 20/40 or better for each eye, with no more than two-lines of difference on the testing chart between eyes to avoid underlying eye dominance. The median visual acuity for both eyes in the participant pool was 20/20. Stereo vision was evaluated using the Titmus Stereoacuity Test (Stereo Optical, Chicago, IL) with an inclusion criteria of 7/9 targets correctly identified in a sequential manner. This corresponded to an angle of stereopsis of 60 s at 16 inches. The median result across participants was 9/9. Both assessments were conducted by the experimenters in well-lit conditions and followed standard testing distances provided by the manufacturers. The demographic and visual screening information for all participants (n = 28) are listed in Table 1.

METHOD DETAILS

Experimental design

The methods closely followed those previously reported[76] and are illustrated in Figure 1. BR was induced using a black opaque divider placed between the eyes, combined with MEG-compatible prism lenses of 12 diopters. The combination of viewing distance and prism strength allowed appropriate fusion of images between the eyes. Before MEG data acquisition, participants practiced the task on a laptop for 5 minutes to become familiar with the experimental procedure.

Participants were instructed to report their visual percepts (red, green, or mixed) using a two-button press-and-hold system. They pressed the button corresponding to their dominant percept (red or green) when it was perceived for at least 80% of the stimulus

square area, holding the button to indicate dominance. These instructions were consistent across testing conditions, and participants were unaware of whether they were in a BR or BR-replay block.

Each experimental run lasted 5 minutes and consisted of four counterbalanced 75-s blocks. Counterbalancing was used for the orientation and color of the orthogonal gratings shown to each eye to mitigate adaptation effects. Participants fused on a fixation screen before each block and initiated the experiment via a button press.

As a control, the BR-replay condition, also termed "simulated rivalry", used software-driven perceptual alternations. Identical stimuli were presented to both eyes, with the software switching between matching red and green colored orthogonal gratings at random time intervals between 1.5 and 3.5 s to match typical BR alternation rates obtained from a prior testing day.[76] The control condition exclusively modeled dominant percept alternations (i.e., red and green), minimizing the likelihood of reporting mixed percepts. The replay was "tagged" using unique stimulus flicker frequencies of 5 Hz for red and 6.67 Hz for green, to mark related MEG source signals, with data collected on a separate MEG testing day.

Visual stimulus

Visual stimuli were presented using Psychtoolbox-3[74,75] and MATLAB 2021a (MathWorks, Natick, MA), as illustrated in Figures 1A and 1B. Stimuli were displayed using a VPixx projector (VPixx Technologies, Saint-Bruno, QC) with a 60 Hz refresh rate. The stimuli consisted of 7 red or green orthogonal gratings shown to each eye, with RGBA values chosen to balance the strength of the stimuli ([0.5 0 0 0.35] for red, and [0 0.35 0 0.35] for green). Grating orientations differed by 90° between eyes, and a central fixation mark was used to increase stability and reduce eye movement during BR.[77] Black borders provided additional cues to aid fusion and maintain fixation. The projector was placed 52 cm away from the prism lenses, with the inner square of stimuli measuring 7.5 cm, corresponding to a visual angle of 8° 14′ 0.97''.

MEG data collection

MEG data were collected at the McConnell Brain Imaging Center of McGill's Montreal Neurological Institute using a 275-channel CTF/VSM MEG system (CTF MEG Neuro Innovations, Inc., British Columbia, Canada) with a sampling rate of 2400 Hz. Individualized head models were created by digitizing 100–150 points across the scalp, along with anatomical landmarks and head-position coils using a Polhemus Fastrak system (Polhemus, Vermont, USA). Bipolar signals electrooculogram (EOG), and electrocardiogram (ECG) signals were recorded to capture related artifacts. Empty room recordings were conducted prior to each participant's data collection to capture environmental noise conditions and inform MEG source mapping models. T1-weighted MRI scans (1.5T Siemens Sonata) were acquired for each participant to further inform MEG source mapping.

MEG preprocessing and cleaning

Preprocessing of MEG data was conducted in Brainstorm,[73] which is freely available under the GNU general public license (http://neuroimage.usc.edu/brainstorm), and following good-practice guidelines,[73] as in former MEG BR studies.[16,17] The data was downsampled from 2400 Hz to 600 Hz, and notch filters with a 3-dB notch bandwidth of 2 Hz were applied at 60 Hz, 120 Hz, and 180 Hz to attenuate power line contamination. A high-pass filter at 0.3 Hz was also used to remove the MEG DC offset and slow drifts.

The participants' T1-weighted MRI data was co-registered to MEG channel locations based on the digitized locations of scalp and anatomical fiducial points including nasion, left and right periauricular points.

Data cleaning targeted artifacts such as heartbeats, eye blinks, and muscle activity using signal-space projection (SSP). SSP components were visually examined and removed when accounting for at least 10% of the data variance around each artifact category and displaying related topographies. In all cases, the result of the corrections was visualized and evaluated. Segments with muscle tension or other artifacts during stimulus presentation were also excluded. The first trial from each block was disregarded, due to the uncertain prior perceptual state. Initially, 10,368 button presses were registered across all participants, and 8,930 remained after preprocessing and quality control (86.1% of all original events).

MEG source mapping

We used Brainstorm[73] with default source imaging participant to produce cortical maps of MEG sources. Individual head models were generated using the overlapping spheres method, and unconstrained beamformer models were created, informed by noise (from empty-room data) and data (from epoch data) covariance statistics. MRI segmentation was performed using CAT12[78] and SPM12, available as Brainstorm plug-ins. Source maps were produced from cortical surfaces comprising of 15,000 vertices. The Human Connectome Project (HCP-MMP1) atlas[79] was used to define 25 regions of interest listed in Table 2, each combining right and left hemisphere labels to cover key posterior cortical regions. We defined a hierarchy in the visual system (i.e., early, mid-level, high-level lateral-ventral, and high-level dorsal) based on previous findings that used a combination of MEG and fMRI to record measures of onset and peak latencies,[51] in addition to grouping regions with spatial proximity.

Event related analysis

Alpha-band activity was analyzed in an event-related framework, time-locked to button presses during BR and BR-replay. Three events were analyzed: exclusive dominant percepts in BR, mixed percepts in BR, and exclusive percepts in BR-replay. For all analyses, red and green perceptual reports were grouped together as dominant percepts, while reports of transitioning from red to mixed

or green to mixed were categorized as mixed percepts. Further, the analysis of mixed percepts only included individual events greater than 230 ms in duration. This was performed to mitigate the confounding effects of including very short mixed responses that could be attributed to pre-response reaction time rather than a stable percept and is within the estimated range observed in other studies.[56,80] For all analyses, computations were performed at the individual trial level before averaging across participants. The MEG time series was bandpassed in the 8–13 Hz frequency range, and time-frequency decomposition was computed using Hilbert transform to extract the mean power of the alpha frequency band. Baseline normalization was performed using a *Z* score transformation of the event-related MEG signal power. The baseline period was defined as the time window from 1 to 2 s after the button response. The normalization was applied independently for each participant and across the three conditions (i.e., BR exclusive dominance, BR mixed, and BR-replay exclusive dominance). The normalization procedure provided a standardized scale for analysis across participants and conditions. Event-related analyses were conducted on segments spanning −3 to 3 s relative to button responses, and later extracted between −1 and 1 s, centered around the button responses to minimize the edge effects of the analysis.

Parametrization of the alpha band peak

We isolated the periodic peak components (i.e., the amplitude and peak frequency) of the alpha band oscillations during the BR task for all participant (Figure 3B). This analysis examined individual differences in the peak alpha band activity (8–13 Hz) using spectral parametrization (specparam) methods on the power spectrum density (PSD) analysis for all participants.[50] The Welch method (3 s window length and 50% overlap ratio) was used for the PSD analysis in the primary visual cortex (V1) for all participants. The mean scout function was selected over the both the right and left hemispheres for V1. For the specparam analysis, a frequency range of 1–26 Hz was selected to identify a single peak during the BR experiment. The hyperparameters for this method were a minimum peak height of 0.3 dB and peak width limits of 0.5–3 Hz.

Time-resolved correlation analysis

Correlation analyses were conducted to examine the relationship between alpha band power (8–13 Hz) in the primary visual cortex (V1) and behavioral percept durations. For each participant, the mean baseline normalized (*Z* score) MEG alpha power computed from the Hilbert Transform analysis was extracted from the V1 region (Table 2) across a 2 s time window, from −1 to +1 s, centered around the button response for dominant (i.e., red and green), and mixed percepts. Durations for dominant and mixed percept were derived from the behavioral task, as described above. Analyses were performed in the statistical software R[81] (R Foundation for Statistical Computing, Vienna, Austria), and outlier detection (>3 standard deviations from the group mean) excluded 1 participant from Figures 7B and 2 participants from Figure 7C. At each time point, Pearson correlation coefficients were computed between alpha band power in V1 and mean percept durations, separately for dominant and mixed percepts. To correct for multiple comparisons across the time series, non-parametric permutation testing (1000 iterations) was applied. At each time point, the observed correlation coefficients were compared against a null distribution to obtain permutation-corrected *p*-values.

Directed connectivity analysis

We conducted connectivity analysis using phase transfer entropy (PTE)[82–84] on alpha band activity during dominant percepts. Directed phase transfer entropy (dPTE) between all pairs of ROIs (mean dPTE values across all combinations of the three source time series at each cortical locations, resulting in a 25 × 25 connectome across all pairs of ROIs) was computed with the goal of distinguishing feedback and feedforward connectivity patterns during perceptual dominance. Connectivity analysis was conducted on individual source reconstructions, resulting in group-level measures that provided insight into connectivity between visual areas before and after perceptual dominance.

QUANTIFICATION AND STATISTICAL ANALYSIS

Psychophysics

The statistical analysis for the behavioral results were performed in R.[81] The button-responses for dominant and mixed percepts were analyzed from 28 participants ($n = 28$) during BR and BR-replay. The alternation rates were computed using the total number of dominant button responses and the experiment duration. Percept durations were defined as the sustained response of dominant and mixed percepts, and percept proportions represent an overall viewing percentage of red, green, and mixed responses over the course of the experiments. The psychophysics results were summarized using the mean and 95% confidence intervals in Figure 2. Additionally, standard deviations are reported in the results for psychophysics.

Event-related MEG alpha band power

The alpha band power (8–13 Hz) recorded with MEG from all 28 participants ($n = 28$) was baseline normalized using a *Z* score transformation prior to computing group averaged results. The transformation provided a standardized measure across participants. Event-related MEG results (Figures 5 and 6) excluded mixed percept responses shorter than 230 ms. The results plotted in Figure 5 include the mean baseline normalized alpha band power for dominant and mixed percepts during BR, as well as dominant percept during BR replay. Shaded error regions represent the standard error of the mean (SEM) across participants.

Statistical analyses were conducted in R[81] to assess latency of the alpha band drop prior to dominant percepts during BR and BR-replay (Figure 5). For each participant ($n = 28$), the latency of the lowest alpha power (minimum Z score value) was identified within the time window of −1 to 0.5 s. The results section reports the mean, standard deviation, and effect size (Cohen's d) for the peak latency difference between conditions. A paired t test revealed a significant difference ($t = 2.67$, $df = 27$, $p = 0.013$), with early pre-switch alpha decrease during BR.

To compare the time-resolved alpha power between dominant and mixed percepts during BR (Figure 5A), a two-tailed paired Student's t test ($n = 28$) was performed with a significance threshold of $\alpha = 0.05$. False discovery rate (FDR) correction was applied to account for multiple comparisons across the time series. The analysis was performed in Brainstorm.[73]

Time-resolved correlation analysis

The correlation between baseline normalized (Z score) alpha band power in the primary visual cortex and percept duration is shown in Figure 7. The alpha band power in V1 was extracted for all 28 participants, and cleaning was applied to detect outliers exhibiting mean values more than 3 standard deviations from the group mean. For each time point within the window of −1000 to 1000 ms around the report of alternation, Pearson correlation coefficients were computed between the alpha band power in V1 and the duration of dominant percepts (Figure 7A, $n = 28$), and mixed percepts (Figure 7B, $n = 27$). Clusters of significant time points ($p < 0.05$) were identified and correction for multiple comparisons was applied. To correct for multiple comparisons across the time-series, we performed non-parametric permutation testing (1,000 iterations). At each time point, the correlation coefficients were compared against a null distribution to obtain permutation corrected p-values. The result for individual participants ($n = 26$) is plotted in Figure 7C. 95% confidence intervals were used as the measure of dispersion. The analysis was performed in R.[81]

Connectivity analysis

The directed phase transfer entropy (dPTE) analysis is shown in Figure 8. Alpha band connectivity was assessed between 25 regions of interest listed in Table 2. Patterns of connectivity were evaluated for pre- and post-switch time periods during BR dominant percepts. The analysis was performed for all 28 participants ($n = 28$), prior to computing the group mean results. The Shapiro-Wilk test revealed a non-normal data distribution ($p < 0.05$), therefore non-parametric statistical testing was applied. Significance was assessed at $\alpha = 0.05$ using the paired-sample Wilcoxon signed-rank test (10,000 permutations) with the results shown in Figure 8D. The dPTE analysis and statistical testing for connectivity was performed in Brainstorm.[73]